Molecular Mechanisms of TanshinoneIIA in Hepatocellular carcinomatherapy via WGCNA-based Network Pharmacology Analysis

Han Zhao (zhaohan@mail.ustc.edu.cn)
Jianghan University https://orcid.org/0000-0002-5127-8112
Jing Guo
Jianghan University
Qingjia Chi
Wuhan University of Technology
Meng Fang
Jianghan University

Research

Keywords: Tanshinone IIA, Hepatocellular carcinoma, Network pharmacology, WGCNA, Molecular docking

Posted Date: January 29th, 2021

DOI: https://doi.org/10.21203/rs.3.rs-154091/v1

Abstract

Background: Hepatocellular carcinoma (HCC) is a worldwide malignant tumor that caused irreversible consequences. The studies of Tanshinone IIA showed that Tanshinone IIA has played a notable role in HCC treatment. However, it is still to be investigated to discover the potential targets and associating mechanism of Tanshinone IIA against HCC.

Methods: To analyze the correlation between genes and specific clinical features, we applied weighted gene co-expression network analysis (WGCNA), which can help us identify the targets of Tanshinone IIA related to the clinical features of Hepatocellular carcinoma.

Results: We screened out 105 overlapping genes by integrating the predicted targets of Tanshinone IIA and the gene expression profile of HCC from the Cancer Genome Atlas (TCGA) database. For WGCNA, we used the RNA-seq profile of the overlapping genes and the related clinical information of HCC from TCGA. And 23 genes related to clinical tumor grade in the important module (R2 = 0.37) were imported for Gene Ontology (GO) enrichment, Kyoto Encyclopedia of Genes and Genomes (KEGG) analysis and protein-protein interaction (PPI) analysis. Compared to the key genes in the significant module from WGCNA with the high connectivity nodes from the PPI network, we can analyze three hub genes, AURKB, KIF11, and PLK1, for further verification. We tested the binding of Tanshinone IIA to the targets of Hepatocellular carcinoma using Autodock Vina. The survival curve validated that the three hub genes represented a poor prognosis. Receiver operating characteristic (ROC) curves demonstrated that the three hub genes were effective in diagnosis. The mRNA expression of the three hub genes was upregulated in the HCC than the normal. AURKB, KIF11 and PLK1 were further upregulated in advanced tumor stage and grade. Moreover, AURKB, KIF11 and PLK1 also had higher protein expression in HCC tissues.

Conclusions: In the study, WGCNA revealed grade-specific gene modules, indicating that Tanshinone IIA probably plays its therapeutical effect in the differentiation process of HCC. And the study partly interpreted the pharmacological mechanism of Tanshinone IIA against HCC.

Introduction

Hepatocellular carcinoma (HCC), the leading kind of liver cancer, is a heterogeneously distributed malignant tumor [1]. Risk factors, such as chronic hepatitis B/C virus, genetic and epigenetic, have been identified as the cause of HCC [2]. Despite the development of surgical treatment and immunotherapy, the survival rates remain low [3]. HCC had poor prognosis because the recurrence rate and metastasis rate of HCC are very high. Liver transplantation is the most effective approach in liver cancer therapy. However, it is known to us that the donor resource is quite scarce and limited. The continuing high recurrence rate and metastasis rate and inadequate liver function after the operation also challenged the effect of liver transplantation. This makes treatment less curable though it seems that the surgery is considerable success in a sense. Therefore, we must consider many aspects to found a more effective and safer treatment for HCC.

Tanshinone IIA is extracted from chinese medicine Salvia miltiorrhiza Bunge [4]. Studies reported that Tanshinone IIA participates in numerous biological functions, containing widely accepted antiangiogenic function, antioxidant and anti-inflammatory effect, and the new use in anticancer [5]. Studies found Tanshinone IIA inhibits HCC by regulating angiogenesis, proliferation, and apoptosis of tumor cells [6, 7], indicating that Tanshinone IIA can exert anticancer activity probably through a multi-target and multi-pathway pattern. However, the exact targets of Tanshinone IIA are not clear, and so is its anti-HCC mechanism. Thus, it is necessary to reveal and discover the therapeutic target and mechanism of Tanshinone IIA in HCC therapy.

Network pharmacology is becoming a popular approach for drug target prediction against disease [8–10]. It offers a comprehensive sight into the new drug or complex mechanisms of an existing drug against a new disease. Moreover, network pharmacology provides a systematic method to promulgate the interreaction between a drug and a disease via the overlapping genes. By integrating data from databases containing TCMSP, BATMAN-TCM, SymMap, STITCH, SEA, Swiss, and PharmMapper, the Cancer Genome Atlas (TCGA), we obtained the overlapping target genes of Tanshinone IIA against HCC. RNA-seq data of the overlapping genes and the related clinical information of Hepatocellular carcinoma (HCC) from TCGA were used for weighted gene co-expression network analysis (WGCNA), which was an analysis method to set up a gene co-expression network among the interested genes to extract the associations between gene modules and specific clinical properties [11]. To further estimate the genes connections, the genes of the important module were analyzed for the PPI network using Cytoscape. Compared to the key genes from WGCNA with the high connectivity nodes from the PPI network, we screened out the hub genes. Then, we further verified the potential hub targets of Tanshinone IIA against HCC, which had probably interpreted the mechanism of Tanshinone IIA against HCC in a way. Our workflow chart was attached in Fig. 1.

2. Methods

2.1. The ADME-related characters assessment of Tanshinone IIA

As we would use Tanshinone IIA as a drug in HCC disease treatment, we need to evaluate whether Tanshinone IIA has a druggable property at first. From the TCMSP database (https://tcmspw.com/tcmsp.php), we obtained the ADME (abbreviation of absorption, distribution, metabolism and excretion) related properties. We used the concrete parameters including molecular weight (MW), oral bioavailability(OB), intestinal epithelial permeability (Caco-2), blood brain barrier (BBB), drug-likeness (DL), fractional negative surface area (FASA-), the polar surface area (TPSA), and RBN [12]. From which, OB⩾30% and DL⩾0.18 were common used as the criteria to screen out the druggable compounds [13].

2.2. Overlapping target genes of Tanshinone IIA against HCC

First, we identified the targets related to Tanshinone IIA from database. TCMSP (https://tcmspw.com/tcmsp.php), SymMap (https://www.symmap.org/), BATMAN-TCM (http://bionet.ncpsb.org/batman-tcm/) database were searched used the name" Tanshinone IIA". Then we obtained the corresponding "smiles" or 2D/3D structure of Tanshinone IIA from PubChem (https://pubchem.ncbi.nlm.nih.gov/). Then, the targets of Tanshinone IIA were also screened by uploading the required structure to STITCH (http://stitch.embl.de/), SWISS(http://swisstargetprediction.ch/), SEA(http://sea.bkslab.org/) and Pharmmapper (http://www.lilab-ecust.cn/pharmmapper/) database according to their chemical similarity[14–17]. The small molecule of the drug can target specific proteins, and interaction predicted genes were obtained. By removing the duplicated targets, we acquired the predicted targets. Second, we achieved the different expression genes (DEGs) of HCC. We downloaded the whole mRNA expression profile data (372 HCC vs. 50 paracancerous) using SangerBox software (http://sangerbox.com/). Further, we obtained the DEGs between the HCC tissue and paracancerous tissue by edgR analysis. Tanshinone IIA targets and HCC related DEGs were imported to the Venn diagram (https://bioinfogp.cnb.csic.es/tools/venny/) to obtain the overlapping targets. Finally, these overlapping genes were the targets of Tanshinone IIA against HCC used in the subsequent analysis.

2.3 Important module and key genes sorted by WGCNA

WGCNA is a specific technique to analyze the genes correlation with the clinical phenotypes. Here, we used WGCNA to seek for the genes with tumor stage or grade. Preparing the matrix of the RNA-seq of the above 105 overlapping genes at first, the corresponding clinical data were screened according to the expression matrix. The analysis procedure was performed, as described previously[11]. First, the co-expression construction network of overlapping genes; Then, Screening gene modules; Last, identify key genes. Module membership (MM > 0.9) and gene significance (GS > 0.3) represent the importance of genes included in modules and the degree of association between genes and traits, respectively.

2.4 GO and KEGG pathway analysis

From the WGCNA results, we demonstrated the genes in an important module. Furthermore, we performed the important module's genes for functional annotation analysis using DAVID v6.8 (https://david.ncifcrf.gov/). Three terms of GO enrichment were classified into biological process(BP), cell component(CC), and molecular function(MF) to reflect the functional annotation. To understanding the high-level functions of the genes sorted out, we also analyzed KEGG pathways.

2.5 Protein-protein interaction (PPI) analysis

To explore the gene interactions, we input the genes in the important module into the STRING (https://string-db.org/). Though had shown the interaction of the proteins network with nodes and edges in STRING, we still needed visualization and operability of the network. The medium interactions score of > 0.4 were screened for the next visual analysis in Cytoscape3.6.1. We analyzed the network at first after importing the nodes and the interaction information in Cytoscape3.6.1. The information about the degree of the genes represented the genes' connectivity, which reflected the importance of the genes. Genes with a degree above 10 were chosen as high connectivity genes.

2.6 Identify hub genes

By intersecting the key genes in the important modules, with MM > 0.9, GS > 0.3 from WGCNA, and genes with the degree > 10 from PPI network analysis, we obtained the hub genes. The hub genes coming from Tanshinone IIA, meanwhile with the highest correlation with HCC was obtained.

2.7 Molecular docking

Molecular docking was conducted using AutoDock Vina to verify the binding affinity of hub genes to Tanshinone IIA. Molecular docking can help us predict the interaction of the ligand and the macromolecules, providing the possibility that the ligand might be effective on the macromolecular proteins [18–20]. In our work, we predicted the protein molecular (AURKB, KIF11, PLK1) interacted with Tanshinone IIA in the bound state. Firstly, the required lig.mol2 and rep.pdb files were obtained. Download the 3D structure of Tanshinone IIA from Pubchem, saving as lig.mol2. Download the structure of protein molecular from RCSB PDB (https://www.rcsb.org/). PyMOL portable edition was then conducted to remove solvent and organic of the protein molecular, saving as rep.pdb, which was prepared for the second step. Then, the rep.pdb and lig.mol2 files were respectively transformed to rep.pdbqt and lig.pdbqt, meanwhile, the grid.gpf was obtained in AutoDock. At last, we used the three files in step two in Vina docking process, and we visualized the results in PyMOL soon afterwards.

2.8 Validate the hub genes

To further validate the probability, we then collected related information from several databases. UALCAN (http://ualcan.path.uab.edu) is a powerful and comprehensive resource providing the expression of genes, methylation level, and its survival analyses in cancer [21]. ROC curves were plotted with R package to test the diagnostic significance of the hub genes according to the area under curve (AUC) value. Oncomine (www.oncomine.org) is an enormous platform that can analyze gene expression profiles of a specific tumor. Here, we validated the expression of hub genes in different livers using Oncomine

resource. In addition, by comparing the immunohistochemistry slices using the Human Protein Atlas (http://www.proteinatlas.org), we further validated protein expression.

3. Results

3.1. ADME-related characteristic of Tanshinone IIA.

From the TCMSP results, the OB value of Tanshinone IIA is 49.89% and Tanshinone IIA showed a superior DL value 0.40, indicating that Tanshinone IIA can be absorbed effectively and has good druggability. The other properties of Tanshinone IIA, such as MW, AlogP, FASA, TPSA, and RBN were shown (Table 1). Therefore, it is reasonable to use Tanshinone IIA as a drug in HCC treatment.

Table 1
ADME-related properties of Tanshinone IIA

MW	AlogP	OB (%)	Caco-2	BBB	DL	FASA	TPSA	HL
294.3	4.66	49.89	1.05	0.70	0.4	0.31	47.28	23.56

3.2. Overlapping genes of Tanshinone IIA against HCC

We predicted the targets of Tanshinone IIA by TCMSP, SymMap, BATMAN-TCM, STITCH, SWISS, SEA, Pharmmapper servers. The first three databases were searched used the name" Tanshinone IIA", while the last four databases were obtained according to the structure of Tanshinone IIA. The numbers were 38, 25, 7, 9, 100, 20, and 256, respectively. Furthermore, set union and removed the duplicated genes of all the predicted targets, among which we obtained 384 targets for the next analysis. The mRNA related genes were screened out from the downloaded HCC expressed profile. Further, we obtained a total number of 3391 DEGs between the HCC tissue samples and paracancerous tissue using the edgR method. That is to say, the predicted targets of Tanshinone IIA were 384, and there are 3391 DEGs. Then, Venn diagram showed the intersection genes. Finally, 105 overlapping genes were predicted (Fig. 2).

3.3 WGCNA screened important module and key genes

The expression matrix of 105 DEGs overlapping genes and the related clinical data were prepared for WGCNA analysis. With the module selection criteria (cut height: 0.1, minimum module size: 5), we obtained four modules. The correlation between the blue module and tumor grade was the most important (correlation coefficient = 0.37, P = 2e − 13) (Fig. 3). There are 23 genes in the blue module, in which four key genes (PLK1, KIF11, AURKB, EZH2) were contained in the blue module with a strict criterion of MM > 0.9 and GS > 0.3.

3.4 GO and KEGG analysis of blue module

There are 46 terms involved in BPs, 15 terms in CCs and 10 terms in MFs. In details, the BPs were enriched in mitotic nuclear division, G2/M transition of mitotic cell cycle, cell division, cell proliferation, regulation of cell cycle, spindle organization, response to drug, etc. The CCs were enriched in cytosol, spindle microtubule, nucleoplasm, spindle midzone, nucleus, and chromosome passenger complex,etc. The MFs were enriched in protein kinase binding, protein kinase activity, kinase activity, ATP binding, phosphoprotein phosphatase activity, drug binding, protein serine/threonine kinase activity, etc. From which, we showed the top 10 of BPs, CCs and MFs, respectively (Fig. 4 and Table 2). KEGG pathway analysis showed seven enriched pathways (Fig. 5, Table 3), involving in the cell cycle, progesterone-mediated oocyte maturation, MicroRNAs in cancer, pyrimidine metabolism, viral carcinogenesis, etc. (Table 3). Then, we analyzed the drug-target-pathway interactions (Fig. 6A), and showed the pathway of the cell cycle (Fig. 6B).

Table 2
GO enrichment analysis ($p < 0.05$)

Category	Term	Count	PValue
GOTERM_BP_DIRECT	GO:0007067 ~ mitotic nuclear division	8	1.99E-08
GOTERM_BP_DIRECT	GO:0000086 ~ G2/M transition of mitotic cell cycle	6	7.91E-07
GOTERM_BP_DIRECT	GO:0051301 ~ cell division	7	4.42E-06
GOTERM_BP_DIRECT	GO:0008283 ~ cell proliferation	7	5.71E-06
GOTERM_BP_DIRECT	GO:0051726 ~ regulation of cell cycle	5	1.87E-05
GOTERM_BP_DIRECT	GO:0007051 ~ spindle organization	3	1.94E-04
GOTERM_BP_DIRECT	GO:0042493 ~ response to drug	5	5.95E-04
GOTERM_BP_DIRECT	GO:0097421 ~ liver regeneration	3	6.51E-04
GOTERM_BP_DIRECT	GO:0000079 ~ regulation of cyclin-dependent protein serine/threonine kinase activity	3	0.001179039
GOTERM_BP_DIRECT	GO:0046777 ~ protein autophosphorylation	4	0.001409272
GOTERM_CC_DIRECT	GO:0005829 ~ cytosol	16	3.58E-07
GOTERM_CC_DIRECT	GO:0005876 ~ spindle microtubule	4	1.96E-05
GOTERM_CC_DIRECT	GO:0005654 ~ nucleoplasm	13	2.27E-05
GOTERM_CC_DIRECT	GO:0051233 ~ spindle midzone	3	2.35E-04
GOTERM_CC_DIRECT	GO:0005819 ~ spindle	4	4.01E-04
GOTERM_CC_DIRECT	GO:0030496 ~ midbody	4	4.84E-04
GOTERM_CC_DIRECT	GO:0005634 ~ nucleus	15	0.001007924
GOTERM_CC_DIRECT	GO:0032133 ~ chromosome passenger complex	2	0.0060221
GOTERM_CC_DIRECT	GO:0000922 ~ spindle pole	3	0.007573146
GOTERM_CC_DIRECT	GO:0045120 ~ pronucleus	2	0.008421234
GOTERM_MF_DIRECT	GO:0019901 ~ protein kinase binding	8	3.29E-07
GOTERM_MF_DIRECT	GO:0004672 ~ protein kinase activity	6	8.27E-05
GOTERM_MF_DIRECT	GO:0016301 ~ kinase activity	5	2.42E-04
GOTERM_MF_DIRECT	GO:0005524 ~ ATP binding	9	3.83E-04
GOTERM_MF_DIRECT	GO:0004721 ~ phosphoprotein phosphatase activity	3	0.001551551

Category	Term	Count	PValue
GOTERM_MF_DIRECT	GO:0008144 ~ drug binding	3	0.004358836
GOTERM_MF_DIRECT	GO:0035174 ~ histone serine kinase activity	2	0.006500008
GOTERM_MF_DIRECT	GO:0004725 ~ protein tyrosine phosphatase activity	3	0.007429052
GOTERM_MF_DIRECT	GO:0004674 ~ protein serine/threonine kinase activity	4	0.012329852
GOTERM_MF_DIRECT	GO:0004712 ~ protein serine/threonine/tyrosine kinase activity	2	0.037142678

Table 3
KEGG pathway analysis

Category	Term	Count	PValue
KEGG_PATHWAY	hsa04110:Cell cycle	7	4.73E-07
KEGG_PATHWAY	hsa04914:Progesterone-mediated oocyte maturation	5	6.38E-05
KEGG_PATHWAY	hsa05206:MicroRNAs in cancer	6	6.57E-04
KEGG_PATHWAY	hsa00240:Pyrimidine metabolism	4	0.002136
KEGG_PATHWAY	hsa04114:Oocyte meiosis	4	0.002797
KEGG_PATHWAY	hsa05161:Hepatitis B	4	0.005934
KEGG_PATHWAY	hsa05203:Viral carcinogenesis	4	0.015293

3.5 PPI network of the blue module

The network of 23 genes from STRING was saved and visualized in Cytoscape 3.6.1. From the network analysis, we chose the parameter of the degree as a screen criterion. Genes with a degree above 10 were regarded as high connectivity genes in the network. As a result, 10 genes met the requirement. The PPI network was shown in Fig. 7.

3.6 Identify the hub genes

We obtained the final hub genes from the intersection between the four key genes from the blue module and the ten genes with a degree above 10 from PPI network analysis, namely PLK1, KIF11, and AURKB.

3.7 Molecular docking

The computational docking simulation is based on the structure to explore the interplay between ligand and proteins [22]. In this study, there were 20 modes for the interactions between the Tanshinone IIA and a target (AURKB, KIF11 or PLK1) using AutoDock Vina. The first mode with the lowest affinity, which indicated a strong binding capacity between Tanshinone IIA and we chose the candidate targets for further visualization. The affinity is -10.3 kcal/mol between Tanshinone IIA and AURKB. The affinity is -8.8 kcal/mol between Tanshinone IIA and KIF11. The affinity is -10.9 kcal/mol between Tanshinone IIA and PLK1. Then we watched the docking results in PyMOL then (Fig. 8).

3.8 Validation of hub genes

To further validate the importance of AURKB, KIF11, and PLK1, we explored the mRNA expression, protein levels, survival curve, and ROC curve. Compared with the normal tissues, the mRNA expression of AURKB, KIF11 and PLK1 was increased in the HCC as shown by UALCAN (Fig. 9A). The DNA methylation levels of AURKB, KIF11, and PLK1 were decreased in cancer (Fig. 9B). By comparing the survival curves, the three hub genes showed a significant prognostic effect for HCC (Fig. 9C). The expression levels increased in the advanced tumor stages and pathological grades (Fig. 10). Time-dependent ROC curves of AURKB (1 year AUC = 0.674, 3 years AUC = 0.616, 5 years AUC = 0.579) KIF11 (1 year AUC = 0.711, 3 years AUC = 0.645, 5 years AUC = 0.586) and PLK1 (1 year AUC = 0.735, 3 years AUC = 0.667, 5 years AUC = 0.611) were drawn from the TCGA database (Fig. 11). ROC curve indicated that AURKB, KIF11, and PLK1 demonstrated good diagnostic biomarkers. The gene expression levels were also validated using Oncomine4.5 platform. As a result, the expression was increased significantly in the five cancer livers than the normal (Fig. 12). Besides, we validated the protein levels using the HPA database, and the cancer tissues showed stronger immunohistochemical staining (Fig. 13).

4. Discussion

In our work, we predicted the targets of Tanshinone IIA, and then analyzed HCC-related DEGs. Further, we imported the 105 overlapping genes between Tanshinone IIA and HCC-related DEGs to construct a co-expression network for sorting important modules and key genes. Then, WGCNA results and PPI network analysis screened out AURKB, KIF11, and PLK1. Then, the validation of the hub genes was conducted by molecular docking, the expression level, the prognostic significance, diagnostic value, and the protein level. In total, we revealed that Tanshinone IIA had exerted a protective role in the HCC therapy.

Studies have reported that Tanshinone IIA promoted cell death and apoptosis of HCC. For instance, Tanshinone IIA treatment resulted in cell death through the p53 involved pathway in HCC [6]. Tanshinone IIA usage and sorafenib or its combined derivative therapy promoted the caspase activation and inhibited the cell migration and invasion [23]. Tanshinone IIA also induced apoptosis and necroptosis by inhibiting the specific protein activities from protecting HCC [7]. Tanshinone IIA induced apoptotic cell death by inhibiting CYP2J2 activity [24]. In vivo study demonstrated that Tanshinone IIA prevented HCC J5 cell growth in caspase three dependent apoptosis and CD31 related immune reaction [25]. Besides,

Tanshinone IIA also induced calcium-dependent apoptosis [26]. The studies suggested that previous studies focused on cell death and apoptosis. However, does Tanshinone IIA exert its protective role in the opposite way, such as inhibiting cell proliferation? It provided us an opposite thought about Tanshinone IIA against HCC, though the direct evidence is little. GO and KEGG pathway results demonstrated most genes in the important module screened by WGCNA were involved in the cell cycle, a pathway that the Tanshinone IIA probably acted through.

The analysis results suggested that AURKB, KIF11, and PLK1 are hub targets that Tanshinone IIA binding. AURKB (Aurora kinase B) is a mitotic kinase involved in the mitotic process, especially in various cancers, such as clear cell renal cell carcinoma [27], chronic myeloid leukemia [28], acute lymphoblastic leukemia [29], and HCC [30]. The selective AURKB inhibitor was evaluated as a treatment in human HCC cell lines [31]. KIF11 (kinesin family member 11), a member of the kinesin family, participates in chromosome navigation in the cell cycle [32, 33]. Recent studies have demonstrated that kinesins might act as oncogenes in several cancer types [32, 34, 35]. Silencing KIF11 with a specific small-molecule inhibitor would block the glioblastoma cells' proliferation and reduced invasion in glioblastoma [36]. Even targeting kinesin therapy for tumor have conducted [37]. PLK1 (Polo like kinase 1), a Ser/Thr kinase, plays a pivotal role in cell division [38]. PLK1 played a role in cancer development and progression, such as breast cancer, ovarian cancer, lung cancer [39–41]. PLK1 presented abnormal increase in HCC [39, 42]. Moreover, PLK1 is involved in regulating the cell cycle and apoptosis [43]. Our results indicate that AURKB, KIF11, and PLK1 were abnormally increased in HCC samples. The hub genes screened out were largely associated with the cell cycle, indicating that Tanshinone IIA might exert a protective effect in HCC therapy by regulating the cell cycle. The three hub genes were identified as treatment targets of Tanshinone IIA against HCC by WGCNA prediction and further verification. However, some genes in the other modules analyzed by WGCNA may also be effective in HCC therapy.

In our work, we chose seven database to predict the targets of Tanshinone IIA, so the predicted targets were very comprehensive. However, the HCC-related DEGs used above were only downloaded from the TCGA database, so the gene expression data from Gene Expression Omnibus (GEO) were also downloaded (GSE101685, GSE117361, GSE101728) for supplementary notes. In the three GEO data, we obtained 1958 DEGs genes. The 77 overlapping genes (Figure S1) between Tanshinone IIA and HCC-related DEGs from GEO were imported into Cytoscape for the following PPI analysis. By analyzing the network, we calculated the degree of each node Then. Results showed that overlapping genes involving ALB, ESR1, AR, IGF1, CCNA2, CYP3A4, PLK1, CCNE1, FOS, EZH2, CYP1A1, AURKA, TYMS, REN, CDC25A, CHEK1, CYP1A2, JAK2, CCNE2, AURKB, KIF11 have a degree above 10 (Figure S2(A)). Topology analysis was carried out to identify functional clusters of the overlapping genes in the co-expression network by the plug-in MCODE. According to previous research, we chose the parameter k-core = 2 to extract subnetwork in the co-expression network [44]. Furthermore, we obtained four subnetworks (Figure S2 (B)). Interestingly, the score of cluster 1 was 11.636, containing the main 12 genes, CCNA2, PLK1, AURKA, CCNE1, CDC25A, EZH2, CHEK1, CDC25C, TYMS, CCNE2, AURKB, KIF11, in which KIF11 was the seed, suggesting that KIF11 may be a hub node in the cluster 1. From the results, we concluded that HCC-

related DEGs from GEO might have similar common essential genes compared with TCGA, though with a different method.

There exist some shortages in our present research. Though we had done the verification of the hub genes from the online database, subsequent experiments should be implemented to validate our findings with/without Tanshinone IIA. Furthermore, we did not explore upstream or downstream of AURKB, KIF11, and PLK1 in HCC. Future studies should investigate the mechanisms of AURKB, KIF11, and PLK1 in HCC cell lines.

5. Conclusion

Our study showed that Tanshinone IIA might inhibit mRNA expression of AURKB, KIF11, and PLK1 to arrest cell cycle for exerting its protective role in HCC, which had partly interpreted the pharmacological mechanism of Tanshinone IIA in HCC.

Abbreviations

HCC hepatocellular carcinoma

TCGA the Cancer Genome Atlas

GO Gene Ontology

KEGG Kyoto Encyclopedia of Genes and Genomes

PPI protein-protein interaction

AURKB Aurora kinase B

KIF11 kinesin family member 11

PLK1 Polo like kinase

ROC Receiver operating characteristic

TCMSP Traditional Chinese Medicine Systems Pharmacology

ADME absorption, distribution, metabolism and excretion

MW molecular weight

OB oral bioavailability

BBB blood brain barrier

DL drug-likeness

FASA fractional negative surface area

TPSA the polar surface area

DEGs different expression genes

MM module membership

GS gene significance

AUC area under curve

BP biological process

CC cell component

MF molecular function

GEO Gene Expression Omnibus

Declarations

Ethics approval and consent to participate

Not applicable

Consent for publication

Not applicable

Availability of data and materials

The datasets used and/or analysed during the current study are available from the corresponding author on reasonable request.

Competing interests

The authors declare that they have no competing interests

Funding

This study was supported by the Scientific Research foundation of Jianghan University (No.2020010).

Authors' contributions

Han Zhao analyzed and interpreted the data of Tanshinone IIA and HCC. Jing Guo was a major contributor in writing the manuscript. Qingjia Chi revised the manuscript. Meng Fang provided the idea of the study. All authors read and approved the final manuscript.

Acknowledgements

Not applicable

References

1. Longerich T. [hepatocellular carcinoma]. Pathologe. 2020;41:478–87.
2. Llovet JM, Zucman-Rossi J, Pikarsky E, Sangro B, Schwartz M, Sherman M, Gores G. Hepatocellular carcinoma. Nat Rev Dis Primers. 2016;2:16018.
3. Torre LA, Bray F, Siegel RL, Ferlay J, Lortet-Tieulent J, Jemal A. Global cancer statistics, 2012. CA Cancer J Clin. 2015;65:87–108.
4. Gao S, Liu Z, Li H, Little PJ, Liu P, Xu S. Cardiovascular actions and therapeutic potential of tanshinone iia. Atherosclerosis. 2012;220:3–10.
5. Shi MJ, Dong BS, Yang WN, Su SB, Zhang H. Preventive and therapeutic role of tanshinone a in hepatology. Biomed Pharmacother. 2019;112:108676.
6. Ren X, Wang C, Xie B, Hu L, Chai H, Ding L, Tang L, Xia Y, Dou X. Tanshinone iia induced cell death via mir30b-p53-ptpn11/shp2 signaling pathway in human hepatocellular carcinoma cells. Eur J Pharmacol. 2017;796:233–41.
7. Lin CY, Chang TW, Hsieh WH, Hung MC, Lin IH, Lai SC, Tzeng YJ. Simultaneous induction of apoptosis and necroptosis by tanshinone iia in human hepatocellular carcinoma hepg2 cells. Cell Death Discov. 2016;2:16065.
8. Boezio B, Audouze K, Ducrot P, Taboureau O. Network-based approaches in pharmacology. *Mol Inform* 2017, *36*.
9. Chen SJ, Cui MC Systematic understanding of the mechanism of salvianolic acid a via computational target fishing. *Molecules* 2017, *22*.
10. Huo MQ, Wang ZX, Wu DX, Zhang YL, Qiao YJ Using co-expression protein interaction network analysis to identify mechanisms of danshensu affecting patients with coronary heart disease. *Int J Mol Sci* 2017, *18*.
11. Chi Q, Geng X, Xu K, Wang C, Zhao H Potential targets and molecular mechanism of mir-331-3p in hepatocellular carcinoma identified by weighted gene co-expression network analysis. *Biosci Rep*

2020, *40*.

12. Ru J, Li P, Wang J, Zhou W, Li B, Huang C, Li P, Guo Z, Tao W, Yang Y, et al. Tcmsp: A database of systems pharmacology for drug discovery from herbal medicines. J Cheminform. 2014;6:13.
13. Tao W, Xu X, Wang X, Li B, Wang Y, Li Y, Yang L. Network pharmacology-based prediction of the active ingredients and potential targets of chinese herbal radix curcumae formula for application to cardiovascular disease. J Ethnopharmacol. 2013;145:1–10.
14. Liu XF, Ouyang SS, Yu BA, Liu YB, Huang K, Gong JY, Zheng SY, Li ZH, Li HL, Jiang HL. Pharmmapper server: A web server for potential drug target identification using pharmacophore mapping approach. Nucleic Acids Res. 2010;38:W609–14.
15. Kuhn M, Szklarczyk D, Pletscher-Frankild S, Blicher TH, von Mering C, Jensen LJ, Bork P. Stitch 4: Integration of protein-chemical interactions with user data. Nucleic Acids Res. 2014;42:D401–7.
16. Daina A, Michielin O, Zoete V, Swisstargetprediction. Updated data and new features for efficient prediction of protein targets of small molecules. Nucleic Acids Res. 2019;47:W357–64.
17. Keiser MJ, Roth BL, Armbruster BN, Ernsberger P, Irwin JJ, Shoichet BK. Relating protein pharmacology by ligand chemistry. Nature biotechnology. 2007;25:197–206.
18. Seeliger D, de Groot BL. Ligand docking and binding site analysis with pymol and autodock/vina. J Comput Aided Mol Des. 2010;24:417–22.
19. Trott O, Olson AJ. Autodock vina: Improving the speed and accuracy of docking with a new scoring function, efficient optimization, and multithreading. J Comput Chem. 2010;31:455–61.
20. Nguyen NT, Nguyen TH, Pham TNH, Huy NT, Bay MV, Pham MQ, Nam PC, Vu VV, Ngo ST. Autodock vina adopts more accurate binding poses but autodock4 forms better binding affinity. J Chem Inf Model. 2020;60:204–11.
21. Chandrashekar DS, Bashel B, Balasubramanya SAH, Creighton CJ, Ponce-Rodriguez I, Chakravarthi B, Varambally S. Ualcan: A portal for facilitating tumor subgroup gene expression and survival analyses. Neoplasia. 2017;19:649–58.
22. Geppert T, Proschak E, Schneider G. Protein-protein docking by shape-complementarity and property matching. J Comput Chem. 2010;31:1919–28.
23. Chiu CM, Huang SY, Chang SF, Liao KF, Chiu SC. Synergistic antitumor effects of tanshinone iia and sorafenib or its derivative sc-1 in hepatocellular carcinoma cells. Onco Targets Ther. 2018;11:1777–85.
24. Jeon YJ, Kim JS, Hwang GH, Wu Z, Han HJ, Park SH, Chang W, Kim LK, Lee YM, Liu KH, et al. Inhibition of cytochrome p450 2j2 by tanshinone iia induces apoptotic cell death in hepatocellular carcinoma hepg2 cells. Eur J Pharmacol. 2015;764:480–8.
25. Chien SY, Kuo SJ, Chen YL, Chen DR, Cheng CY, Su CC. Tanshinone iia inhibits human hepatocellular carcinoma j5 cell growth by increasing bax and caspase 3 and decreasing cd31 expression in vivo. Mol Med Rep. 2012;5:282–6.

26. Dai ZK, Qin JK, Huang JE, Luo Y, Xu Q, Zhao HL. Tanshinone iia activates calcium-dependent apoptosis signaling pathway in human hepatoma cells. J Nat Med. 2012;66:192–201.
27. Wan B, Huang Y, Liu B, Lu L, Lv C Aurkb: A promising biomarker in clear cell renal cell carcinoma. *PeerJ* 2019, *7*, e7718.
28. Zhou X, Ma X, Sun H, Li X, Cao H, Jiang Y, Wang P, Xie S, Li Y, Sun Y. Let-7b regulates the adriamycin resistance of chronic myelogenous leukemia by targeting aurkb in k562/adm cells. Leuk Lymphoma. 2020;61:3451–9.
29. Moreira-Nunes CA, Mesquita FP, Portilho AJS, Mello Junior FAR, Maues J, Pantoja LDC, Wanderley AV, Khayat AS, Zuercher WJ, Montenegro RC, et al. Targeting aurora kinases as a potential prognostic and therapeutical biomarkers in pediatric acute lymphoblastic leukaemia. Sci Rep. 2020;10:21272.
30. Sistayanarain A, Tsuneyama K, Zheng H, Takahashi H, Nomoto K, Cheng C, Murai Y, Tanaka A, Takano Y. Expression of aurora-b kinase and phosphorylated histone h3 in hepatocellular carcinoma. Anticancer Res. 2006;26:3585–93.
31. Aihara A, Tanaka S, Yasen M, Matsumura S, Mitsunori Y, Murakata A, Noguchi N, Kudo A, Nakamura N, Ito K, et al. The selective aurora b kinase inhibitor azd1152 as a novel treatment for hepatocellular carcinoma. J Hepatol. 2010;52:63–71.
32. Rath O, Kozielski F. Kinesins and cancer. Nat Rev Cancer. 2012;12:527–39.
33. Muretta JM, Reddy BJN, Scarabelli G, Thompson AF, Jariwala S, Major J, Venere M, Rich JN, Willard B, Thomas DD, et al. A posttranslational modification of the mitotic kinesin eg5 that enhances its mechanochemical coupling and alters its mitotic function. Proc Natl Acad Sci U S A. 2018;115:E1779–88.
34. De S, Cipriano R, Jackson MW, Stark GR. Overexpression of kinesins mediates docetaxel resistance in breast cancer cells. Cancer Res. 2009;69:8035–42.
35. Lucanus AJ, Yip GW. Kinesin superfamily: Roles in breast cancer, patient prognosis and therapeutics. Oncogene. 2018;37:833–8.
36. Venere M, Horbinski C, Crish JF, Jin X, Vasanji A, Major J, Burrows AC, Chang C, Prokop J, Wu QL, *et al.* The mitotic kinesin kif11 is a driver of invasion, proliferation, and self-renewal in glioblastoma. *Sci Transl Med* 2015, *7*.
37. Liu X, Gong H, Huang K. Oncogenic role of kinesin proteins and targeting kinesin therapy. Cancer Sci. 2013;104:651–6.
38. Sun J, Lv PC, Guo FJ, Wang XY, Xiao-Han; Zhang Y, Sheng GH, Qian SS, Zhu HL. Aromatic diacylhydrazine derivatives as a new class of polo-like kinase 1 (plk1) inhibitors. Eur J Med Chem. 2014;81:420–6.
39. Takai N, Hamanaka R, Yoshimatsu J, Miyakawa I. Polo-like kinases (plks) and cancer. Oncogene. 2005;24:287–91.
40. Ahr A, Karn T, Solbach C, Seiter T, Strebhardt K, Holtrich U, Kaufmann M. Identification of high risk breast-cancer patients by gene expression profiling. Lancet. 2002;359:131–2.

41. Lee SY, Jang C, Lee KA. Polo-like kinases (plks), a key regulator of cell cycle and new potential target for cancer therapy. Dev Reprod. 2014;18:65–71.
42. He ZL, Zheng H, Lin H, Miao XY, Zhong DW. Overexpression of polo-like kinase1 predicts a poor prognosis in hepatocellular carcinoma patients. World J Gastroentero. 2009;15:4177–82.
43. Sun W, Su Q, Cao XK, Shang B, Chen AS, Yin HZ, Liu BL High expression of polo-like kinase 1 is associated with early development of hepatocellular carcinoma. *Int J Genomics* 2014, *2014*.
44. Zhang Y, Li Z, Yang M, Wang D, Yu L, Guo C, Guo X, Lin N. Identification of grb2 and gab1 co-expression as an unfavorable prognostic factor for hepatocellular carcinoma by a combination of expression profile and network analysis. PLoS One. 2013;8:e85170.

Supplemental Data

Table S1 is not available with this version.

Figures

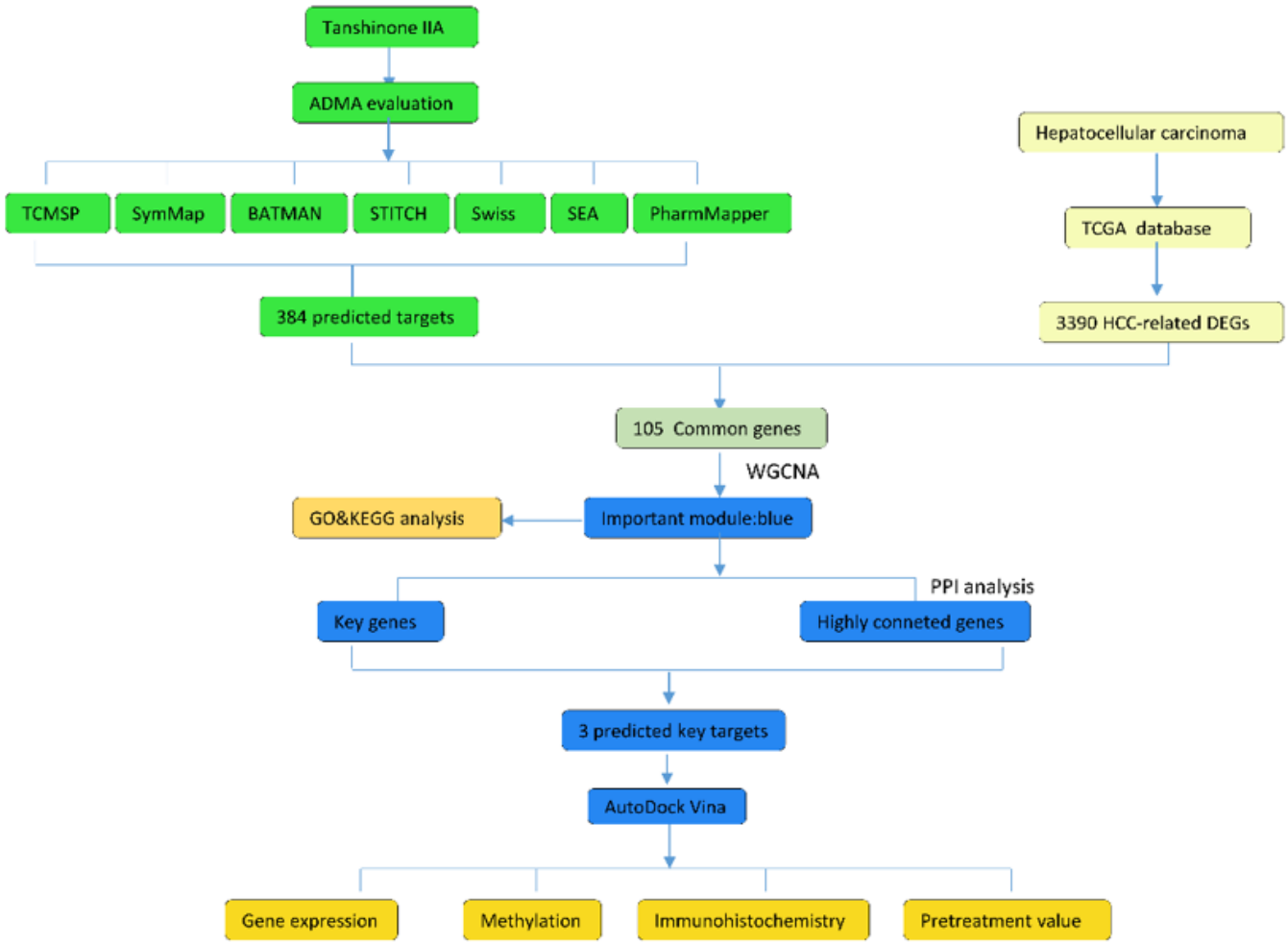

Figure 1

The whole framework of targets prediction and verification. ADME properties of Tanshinone IIA were first evaluated and then potential treatment targets of Tanshinone IIA against HCC were predicted through identifying overlapping genes. Next, WGCNA was analyzed to obtain important module. Then, GO function, KEGG pathway, PPI were performed to predict key targets and their gene function and pathways. Finally, AutoDock Vina molecular docking was conducted. validation were conducted to verify the selected targets and underlying mechanism.

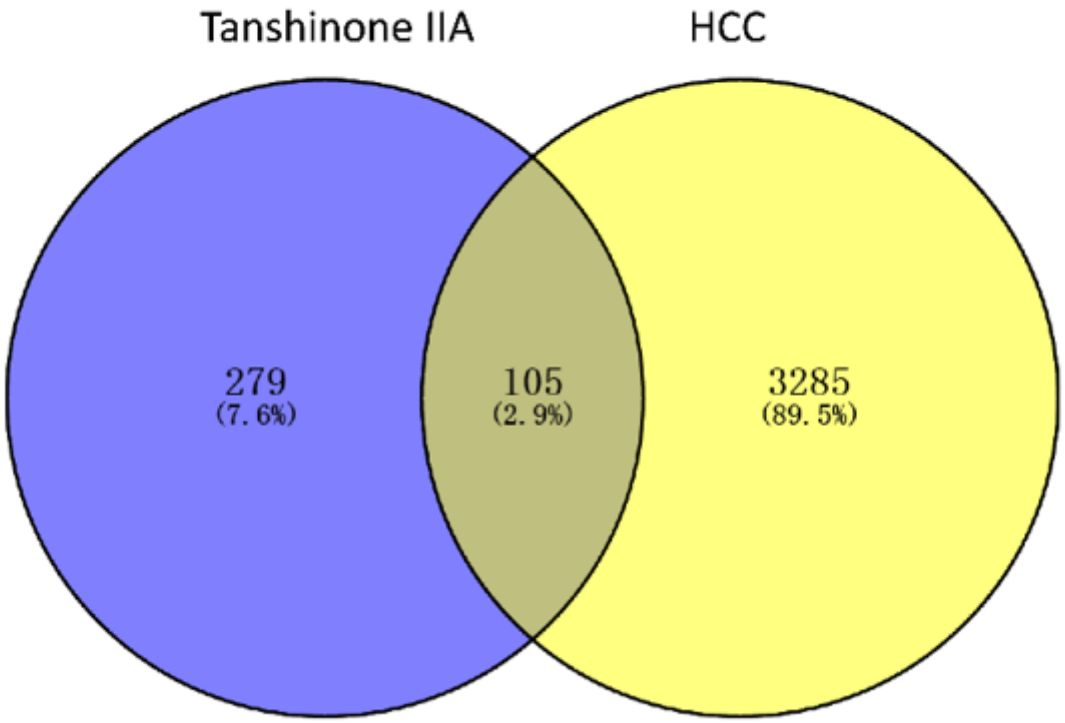

Figure 2

Venn diagram of overlapping genes of Tanshinone IIA and HCC-related DEGs from TCGA. Blue: Tanshinone IIA predicted genes; yellow :HCC-related DEGs in TCGA. Finally, 105 overlapping genes were obtained.

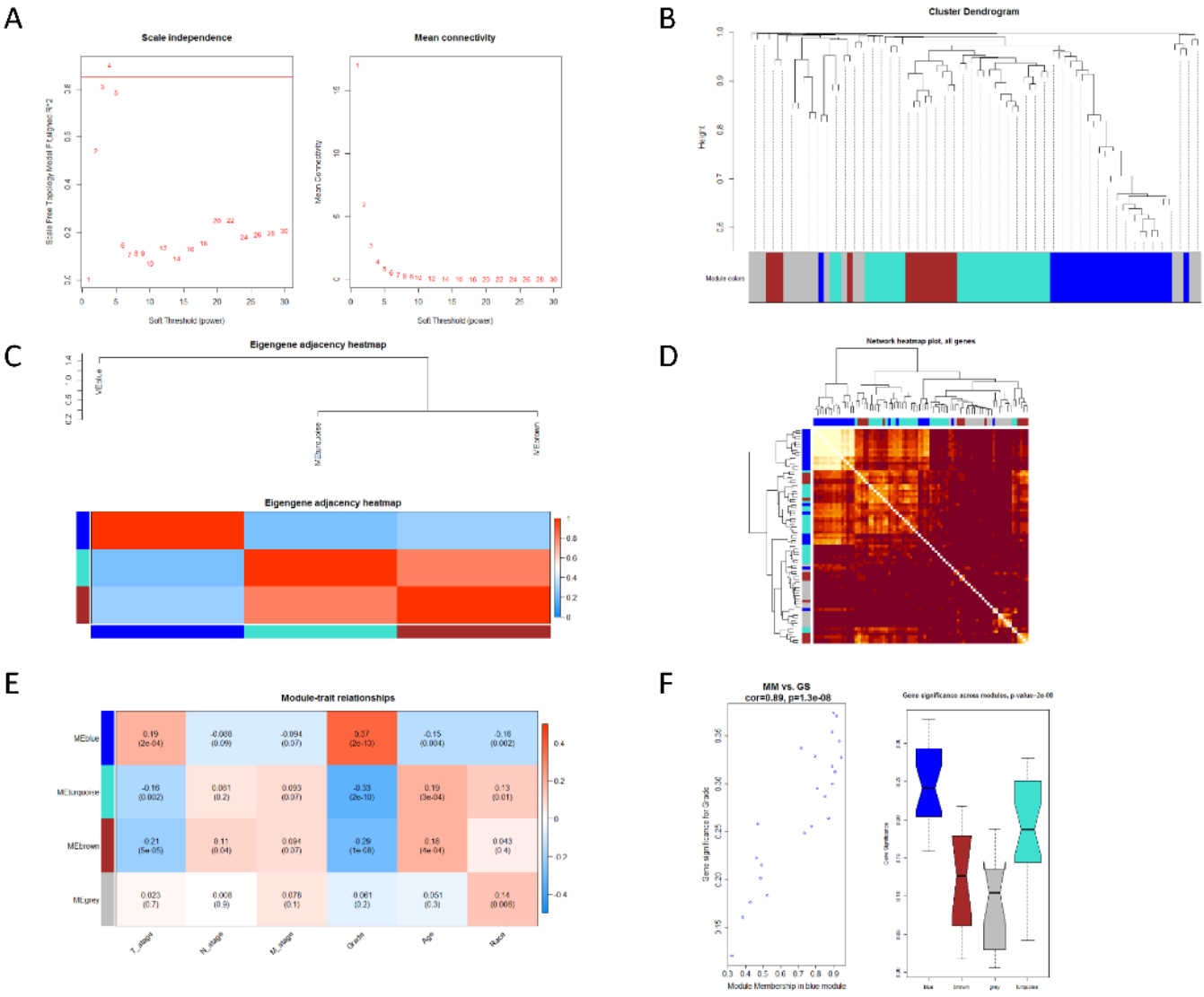

Figure 3

Exploring important modules related to target genes and clinical features through WGCNA. (A) Analyze the scale-free fitting index (left) and average connectivity (right) of various soft threshold weights. (B) Tree map of all DEGs clustered based on dissimilarity measures. (C) Clustering of eigen genes in the module. (D) Correlation between genes. (E) Heatmap of the correlation between modular feature genes and clinical features. Each unit corresponds to a correlation coefficient and a P value. (F) Scatter plot of module eigen genes in blue module and box plot in other module

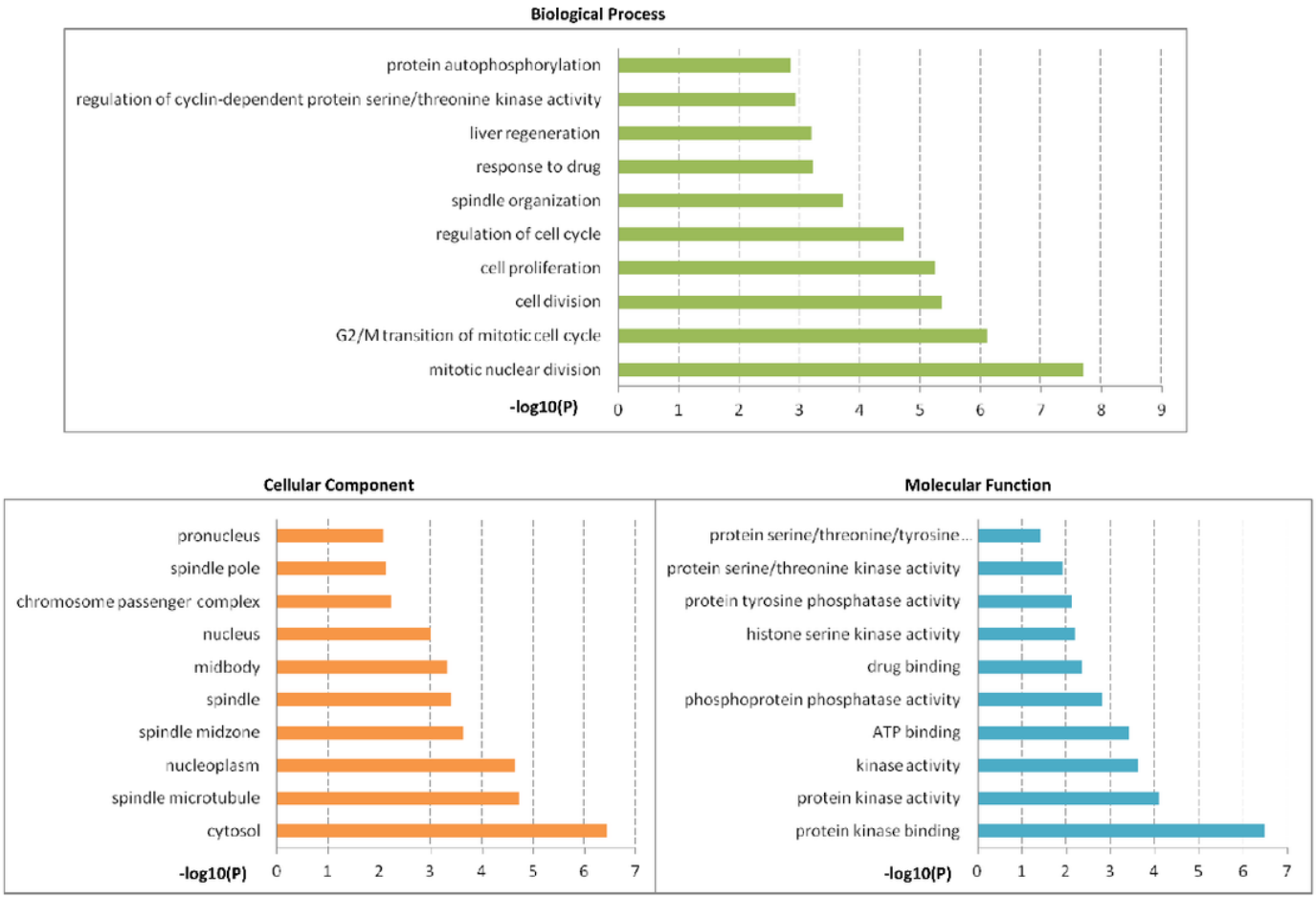

Figure 4

GO enrichment analysis chart, which is divided into biological process, cellular component, and molecular function , and each part is arranged in descending order according to the first 10 terms of Count value ($P<0.05$)

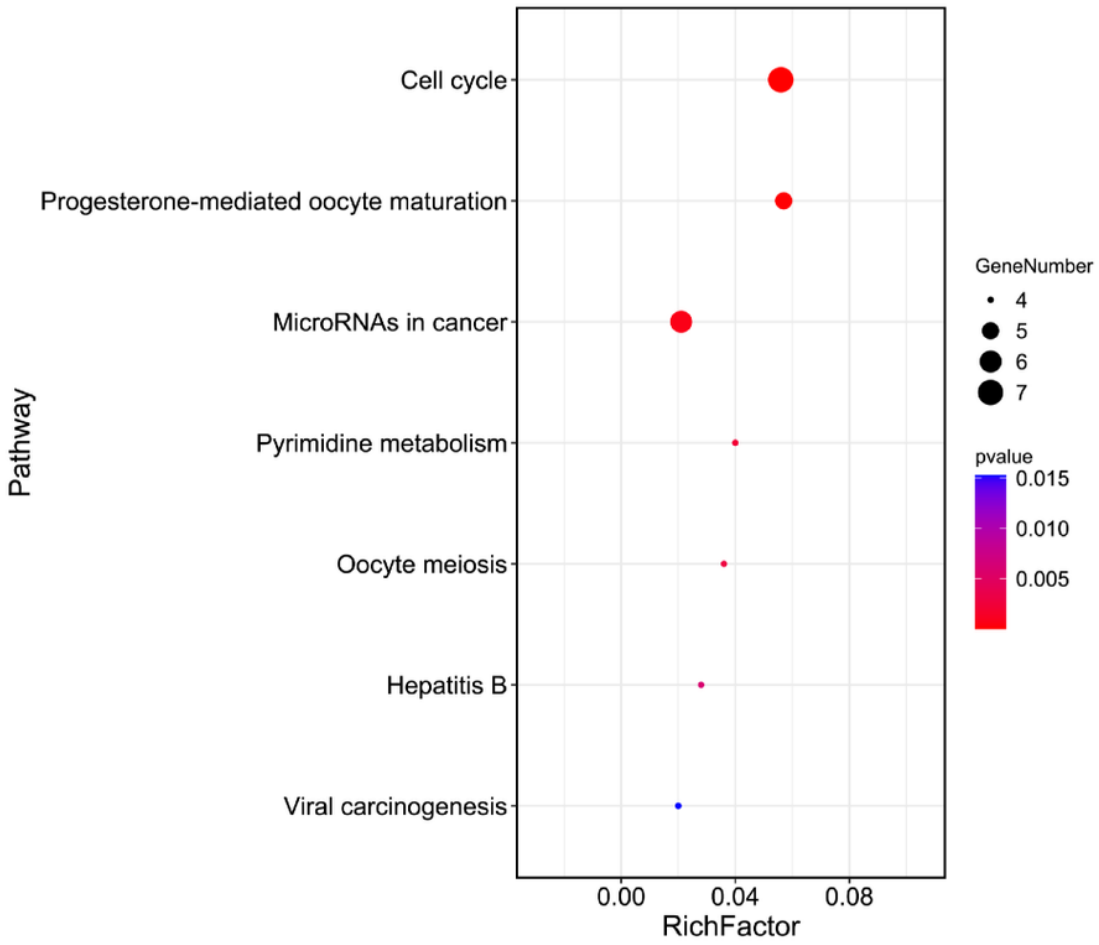

Figure 5

KEGG enrichment analysis. The chart is arranged in descending order of Count value (P<0.05). The larger the bubble, the more the enriched genes contained in the pathway.

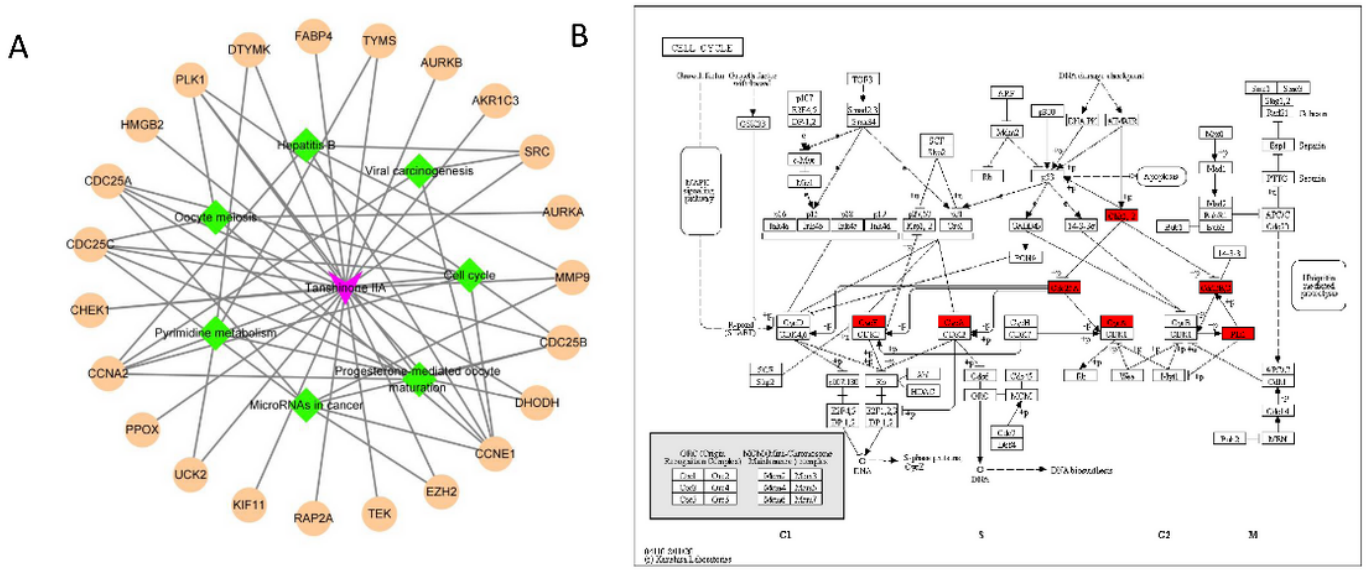

Figure 6

The drug-target-pathway interactions and genes involved in Cell cycle. (A) The drug-target-pathway interactions. (B) Genes involved in Cell cycle.

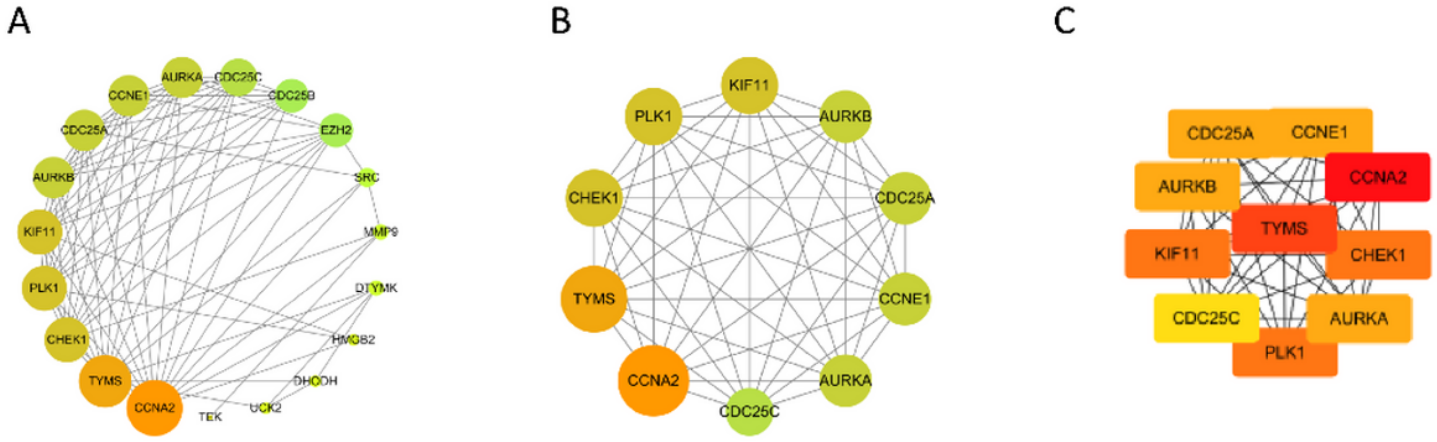

Figure 7

PPI network visualized by Cytoscape. The color of the node changes from orange to green according to the Degree value. The node size changes with the degree value. (A) It showed the whole node of the blue module. (B) Nodes with degree≥10. (C) Cytohubba analyzed top10 genes.

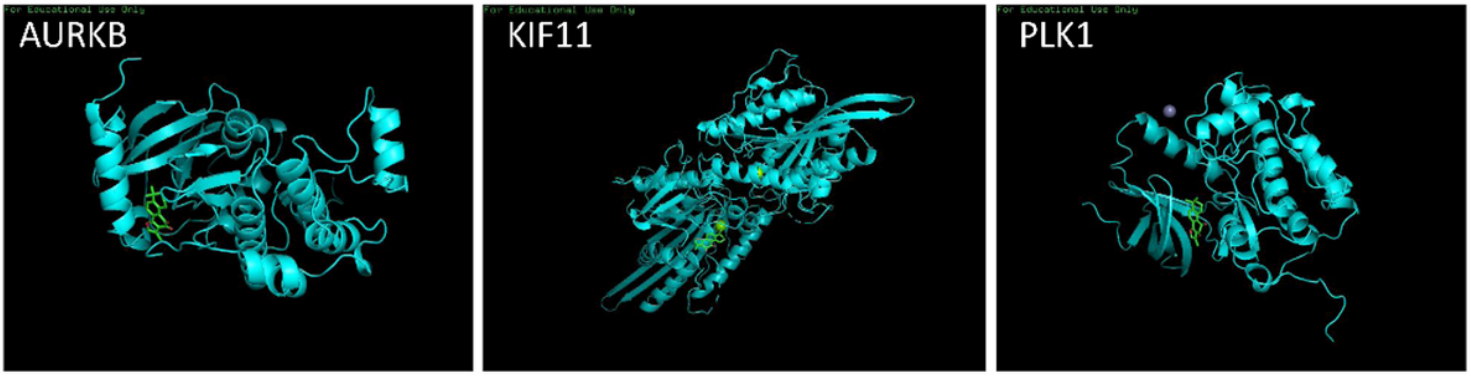

Figure 8

Molecular docking validation by AutoDock Vina. Green is the structure of Tanshinone IIA, cyan represents the target molecular.

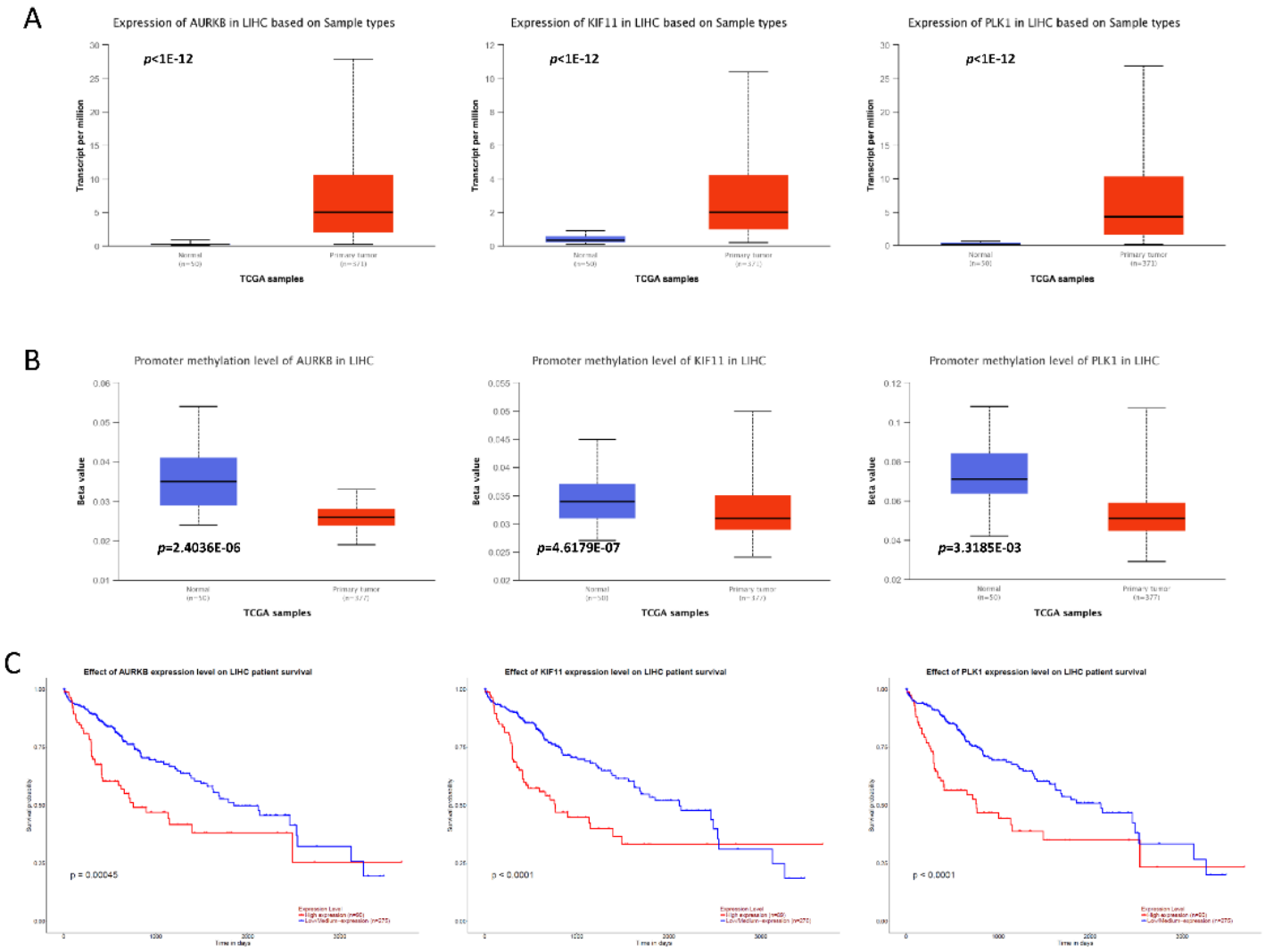

Figure 9

Box plot, methylation analysis and survival curve of gene expression in HCC obtained by UALCAN. (A) Differential expression of AURKB, KIF11, PLK1 in normal tissues and liver cancer tissues. (B) Methylation analysis of AURKB, KIF11, PLK1 in normal tissues and liver cancer. (C) The effect of differential expression of AURKB, KIF11, PLK1 on survival rate of patients with liver cancer.

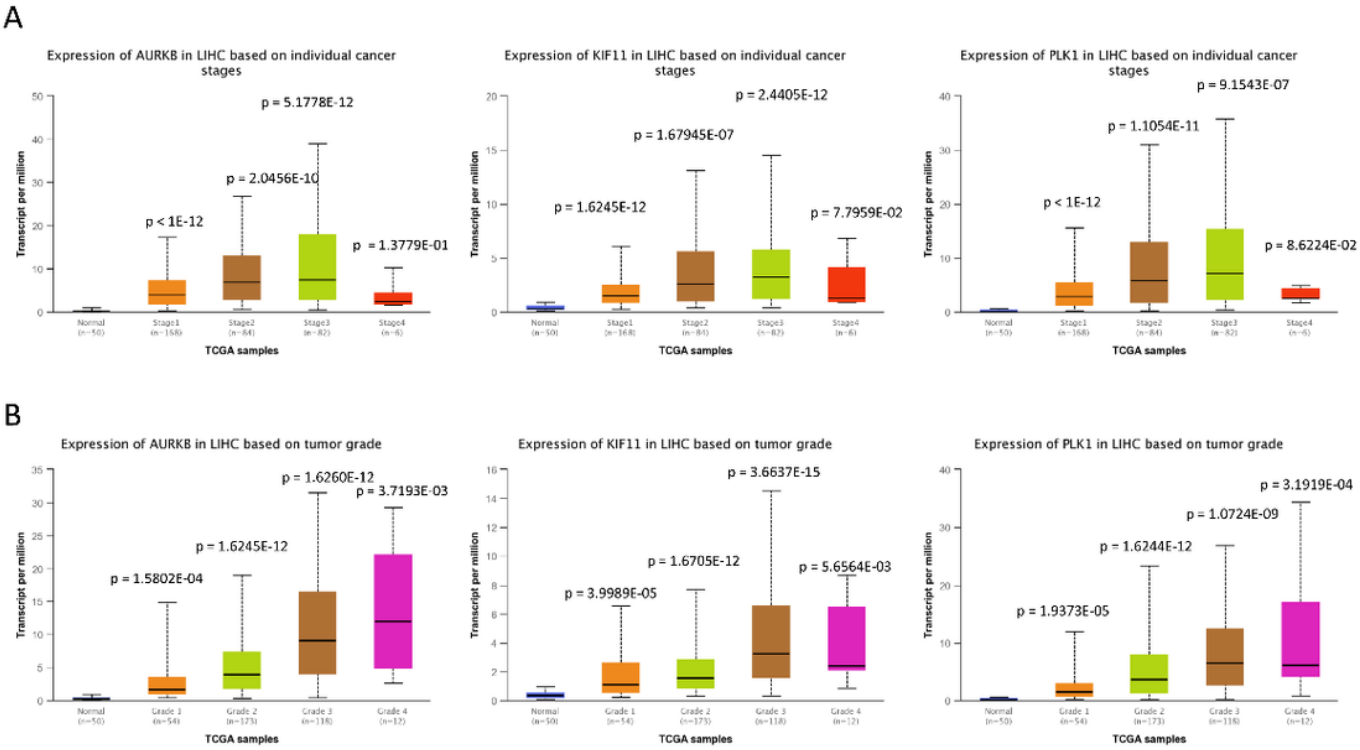

Figure 10

The expression of genes based on individual cancer stage and tumor grade obtained by UALCAN. (A) Differential expression of AURKB, KIF11, PLK1 based on individual cancer stage. (B) Differential expression of AURKB, KIF11, PLK1 based on individual cancer stage .

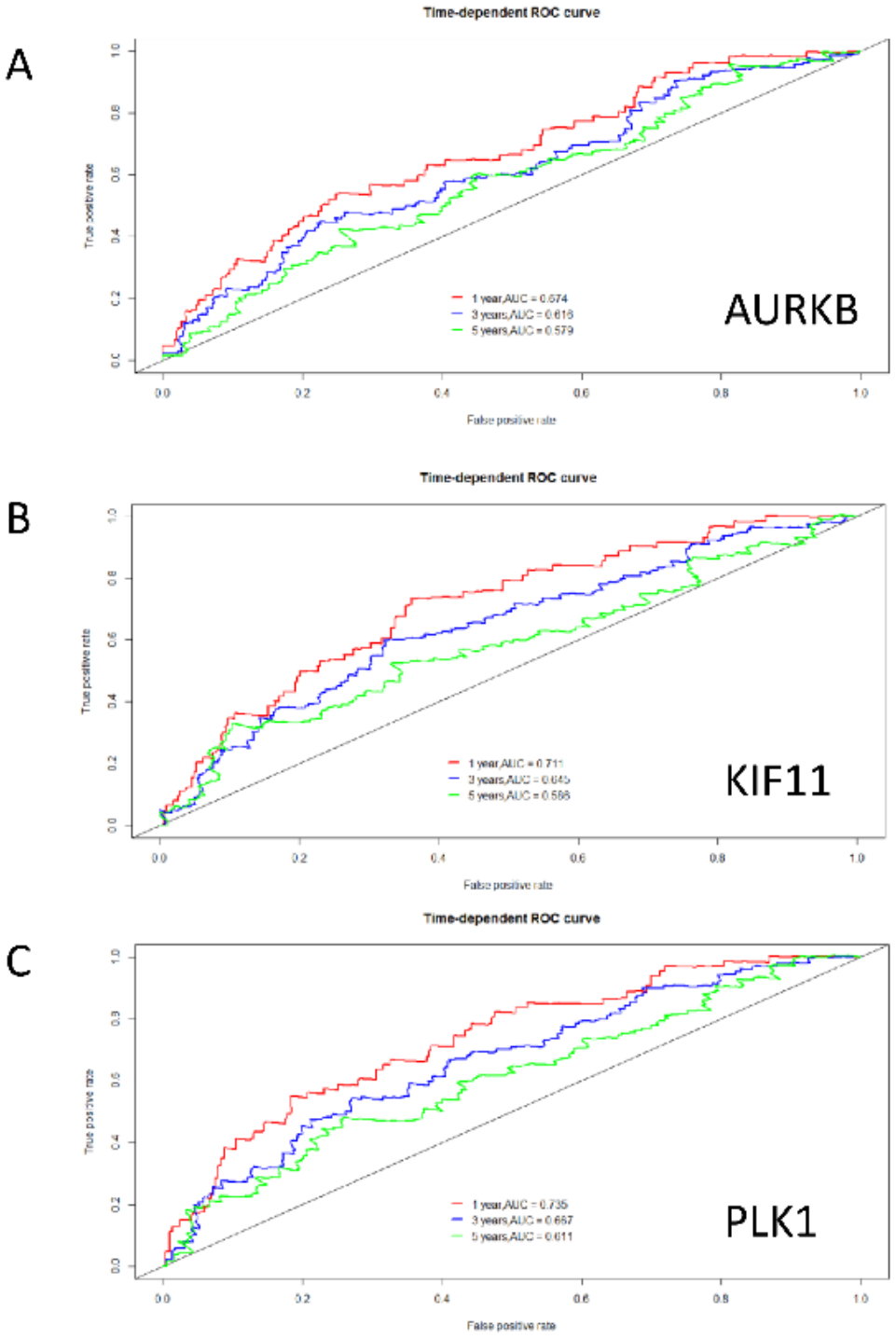

Figure 11

Time dependent ROC curve of hub genes. (A) AURKB (1 year, AUC = 0.674, 3 years, AUC = 0.616, 5 years, AUC = 0.579) (B) KIF11 (1 year, AUC = 0.711, 3 years, AUC = 0.645, 5 years, AUC = 0.586)(C) PLK1 (1 year, AUC = 0.735, 3 years, AUC = 0.667, 5 years, AUC = 0.611).

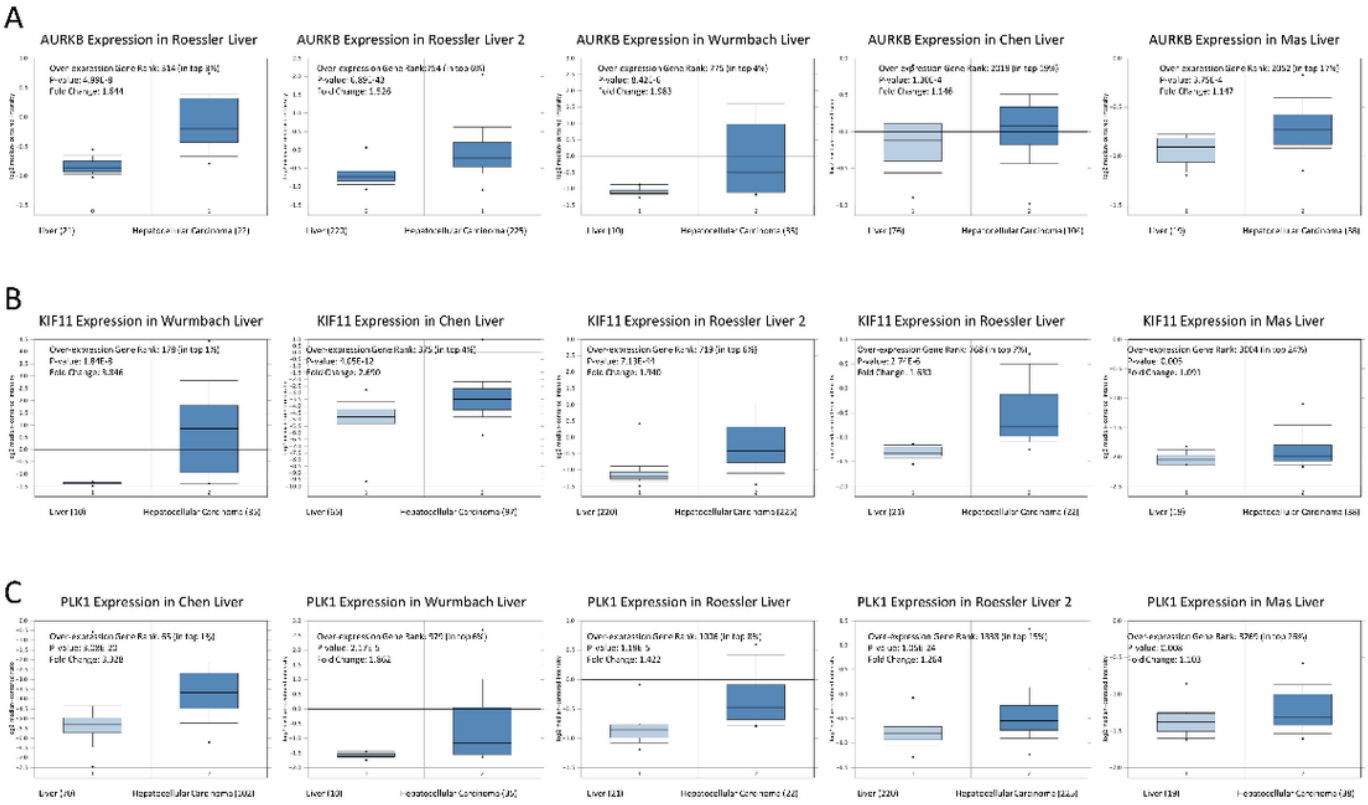

Figure 12

Gene expression in HCC and normal tissues from the Oncomine 4.5 database. (A) Expression of AURKB in different databases. (B) Expressions of KIF11 in different databases. (C) Expressions of PLK1 in different databases. Expressions of these genes were all up-regulated in HCC and had statistical significance for the selected databases ($P<0.05$).

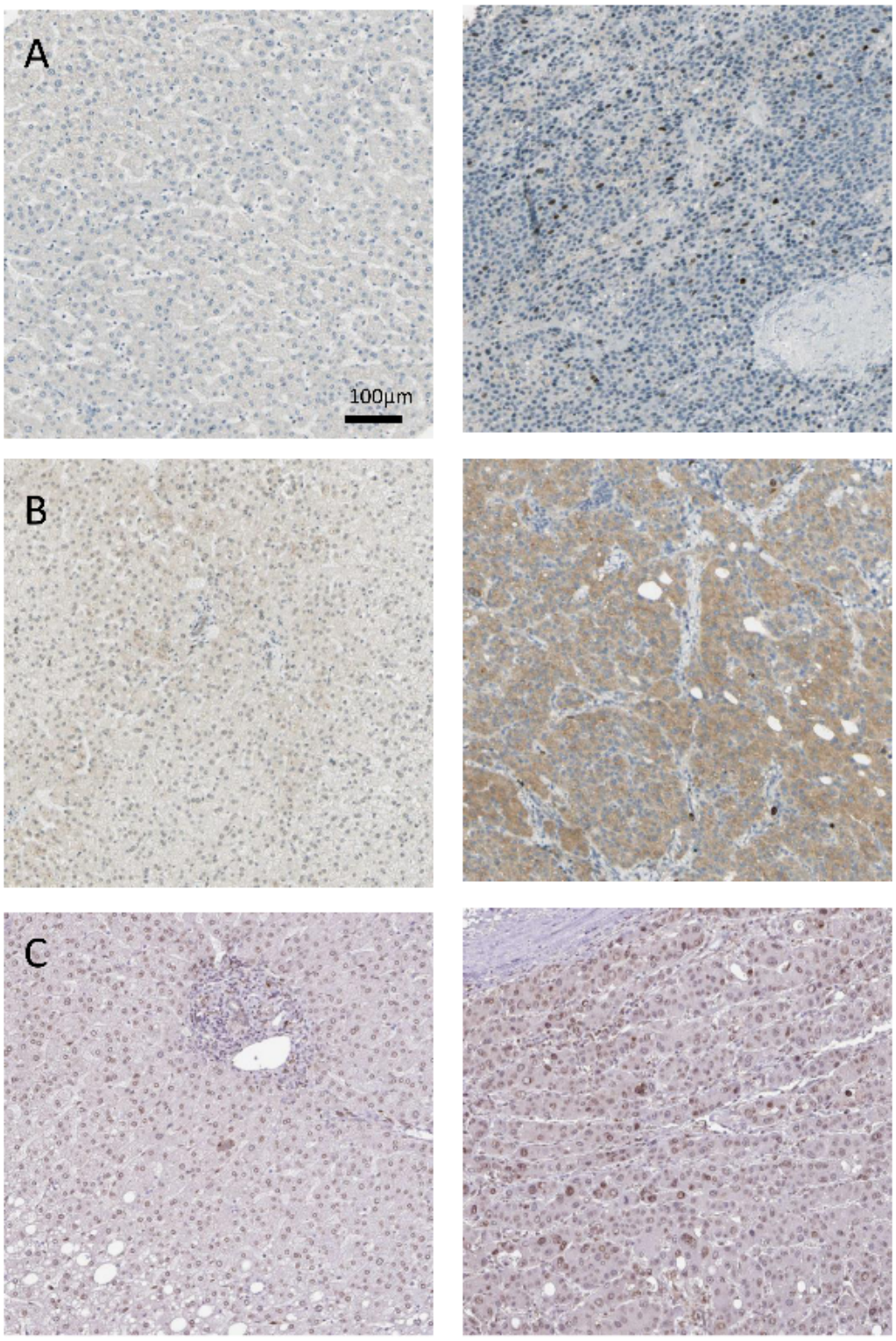

Figure 13

Immunohistochemistry of the three hub genes based on the Human Protein Atlas. (A) Protein levels of AURKB in normal tissue(left panel) and in tumor tissue(right panel). (B) Protein levels of KIF11 in normal tissue(left panel) and in tumor tissue(right panel). (C) Protein levels of PLK1 in normal tissue(left panel) and in tumor tissue(right panel).

Supplementary Files

This is a list of supplementary files associated with this preprint. Click to download.

- Additionalfile1.tif
- Additionalfile2.tif